

## High magnetic-field microwave conductivity of two-dimensional electrons in an array of antidots

P. D. Ye,<sup>1,2</sup> L. W. Engel,<sup>1</sup> D. C. Tsui,<sup>2</sup> J. A. Simmons,<sup>3</sup> J. R. Wendt,<sup>3</sup> G. A. Vawter,<sup>3</sup> and J. L. Reno<sup>3</sup>

<sup>1</sup>National High Magnetic Field Laboratory, Tallahassee, Florida 32310

<sup>2</sup>Department of Electrical Engineering, Princeton University, Princeton, New Jersey 08544

<sup>3</sup>Sandia National Laboratories, Albuquerque, New Mexico 87185

(Received 23 October 2001; published 12 March 2002)

We find the high magnetic field ( $B$ ) microwave conductivity [ $\text{Re}(\sigma_{xx})$ ] of a two-dimensional electron system containing an antidot array increases strongly with frequency ( $f$ ) in the regime with Landau filling  $1/3 < \nu < 2/3$ . At microwave  $f$ ,  $\text{Re}(\sigma_{xx})$  vs  $B$  exhibits a broad peak centered around  $\nu = 1/2$ . On the peak,  $\text{Re}(\sigma_{xx})$  at 10 GHz can be five times its dc-limit value. Unlike the dc-limit conductivity, the microwave conductivity is extremely temperature ( $T$ ) sensitive, increasing as  $T$  decreases down to 100 mK (the lowest  $T$  measured) and disappearing above 0.5 K. The enhanced microwave conductivity is apparently due to antidot edge excitations of fractional quantum Hall effect states, and may be associated with the chiral Luttinger liquids.

DOI: 10.1103/PhysRevB.65.121305

PACS number(s): 73.43.Lp, 73.63.Kv, 78.67.Hc

Collective excitations of a two-dimensional electron system (2DES) patterned with arrays of microscopic, artificial structures, have long been of particular interest since they can be richer than those of unpatterned 2DES, whose long-wavelength dipolar excitations are constrained by Kohn's theorem<sup>1</sup> to show no effect of electron-electron interaction. One role of the artificial structures is to couple electromagnetic radiation to the 2DES at enhanced wave vector,  $q$ , resulting, for example, in the observation of 2D plasmons<sup>2</sup> in far infrared (FIR) optical experiments. In other cases the artificial structures support excitations not easily understood as finite- $q$  plane wave modes of the free 2DES. An array of antidots (small regions from which electrons are excluded) applied to a 2DES exhibits such an excitation,<sup>3</sup> an edge magnetoplasmon encircling the antidots, at much lower frequency than the cyclotron resonance. We now report a microwave-frequency excitation of antidot arrays that occurs *only* in the low temperature ( $T$ ), high magnetic field ( $B$ ) regime of the fractional quantum Hall effect (FQHE).<sup>4</sup>

Patterning 2DES with antidot or other nanostructure arrays has also resulted in striking effects in dc transport. Best known are the commensurability oscillations<sup>5</sup> in low  $B$ , which result from semiclassical ballistic scattering of electrons off the array structures. In an antidot lattice, such "geometric resonance" oscillations appear as resistance peaks at  $B$ 's where the cyclotron orbit of radius  $R_c$  encircles an antidot or group of antidots. In a development of consequence for the understanding of the FQHE, commensurability oscillations have also been observed<sup>6,7</sup> in high  $B$ , near Landau filling  $\nu = 1/2$ . These high- $B$  oscillations are naturally described by composite fermions (CF's),<sup>8,9</sup> exotic particles that contain the electron-electron interaction responsible for the FQHE, and that can (for  $\nu \sim 1/2$ ) be thought of as an electron bound up with two flux quanta. Near  $\nu = 1/2$  the CF's move in an effective magnetic field,  $B_{eff} = B - B_{\nu=1/2}$ , and the resulting CF cyclotron orbits of radius  $R_c = \hbar(4\pi n_s^{1/2})/eB_{eff}$ , where  $n_s$  is the 2DES carrier density, can encircle one antidot or more, resulting in geometric resonance resistance peaks.

This paper presents high  $B$ , finite-frequency measurements of a high mobility 2DES patterned with nanostructure

antidot lattices. The frequency ( $f$ ) is varied between 0.1 and 10 GHz, for temperature  $T \geq 100$  mK, to cover a previously unexplored regime between the dc and FIR experiments. For  $f$  above about 2 GHz, over a broad range of  $\nu$ , centered around  $1/2$ , we find that the measured diagonal conductivity of the array,  $\text{Re}(\sigma_{xx})$ , increases with  $f$ —by as much as a factor of 5 at 10 GHz. Surprisingly, the antidot array in this regime has microwave conductivity *increasing* with  $f$  while *decreasing* with  $T$ . The enhanced microwave conductivity (1) is present only in the FQHE regime  $\nu < 1$ , and at high  $f$  appears in  $\text{Re}(\sigma_{xx})$  vs  $B$  as a striking broad peak roughly symmetric around  $\nu = 1/2$  and (2) requires  $T < 0.5$  K, and increases as  $T$  is reduced down to 100 mK. In contrast, the  $\nu \sim 1/2$  dc-limit conductivity in the same sample is essentially  $T$  independent below 1 K. The stronger  $T$  dependence of the the enhanced microwave conductivity indicates that it is caused by states that do not take part in the dc transport; antidot edge states, that are excited directly by the microwave field would fit this description, and we interpret the data in terms of antidot edge excitations.

Our samples were prepared from GaAs-Al<sub>x</sub>Ga<sub>1-x</sub>As heterojunctions where the 2DES was located approximately 120 nm underneath the sample surface. With the antidots, after low  $T$  red light-emitting diode illumination, carrier density,  $n_s$ , was  $1.1 \times 10^{11}$  cm<sup>-2</sup>. We also measured a reference sample from the same wafer, but without antidots. Without antidots, this wafer had typical 0.3 K electron mobility of around  $\mu \approx 3.6 \times 10^6$  cm<sup>2</sup>/Vs.

Figure 1(a) shows a sketch of the sample with antidots. On its top surface, 200 Å Ti and 3500 Å Au were patterned to form a 2 mm long planar transmission line, consisting of a 30 μm wide center strip separated from side planes by 20-μm-wide slots. These slots contain the antidot array, a square lattice with period  $a = 500$  nm. Holes with diameter 50 nm were defined by electron beam lithography and reactive-ion-beam etching.<sup>10</sup> We report on a sample etched to 50 nm depth; 30 and 70 nm depths gave comparable results. The depleted region around an antidot is much larger than the lithographically defined hole in the wafer; we estimate the depletion region diameter to be 150 to 250 nm. The

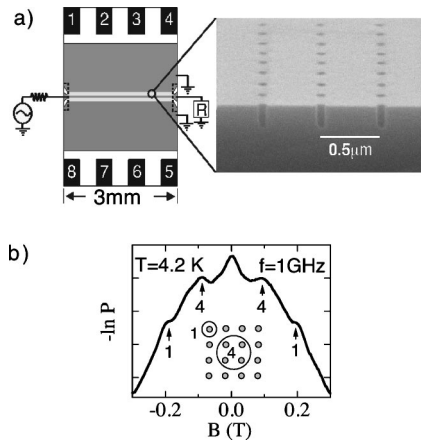


FIG. 1. (a) Top view of sample showing coplanar waveguide transmission line (metal film is dark gray) deposited on top of sample. Ohmic contacts are at the edges (black), and two antidot patterned areas (light gray) are in slots. The right part is a scanning electron micrograph of the antidot array; the array is square but appears foreshortened in one direction because of the angle of view. (b) Microwave absorption for  $a=500$  nm antidot lattice. Geometric resonances due to orbits encircling 1 and 4 antidots are marked.

2DES in the areas enclosed by the dashed lines in Fig. 1(a) was removed by wet etching.

The microwave measurement methods used here are similar to those described in earlier publications.<sup>11</sup>  $\text{Re}(\sigma_{xx})$  is calculated from the effect of the 2DES on microwave propagation through the transmission line which couples capacitively to the 2DES. In the present work, a room-temperature source and receiver are connected to the transmission line by cryogenic coaxial cables.  $\text{Re}(\sigma_{xx})$ , the real part of the diagonal conductivity of the 2DES, is related to the transmitted power,  $P$ ,  $\text{Re}(\sigma_{xx}) = W |\ln(P/P_0)| / 2Z_0 d$ , where  $d=2$  mm is the total length of the transmission line,  $W=20$   $\mu\text{m}$  is the width of a slot,  $P_0$  is the transmitted power for  $\sigma_{xx}=0$ , and  $Z_0$  is 50  $\Omega$ , which is the characteristic impedance for the  $\sigma_{xx}=0$  case. Detailed analysis of the system in the quasi-transverse electric magnetic approximation (including reflections, distributed capacitive coupling, and the effect of the 2DES on the true characteristic impedance of the line) shows an  $f$  (but not  $T$  or  $B$ ) dependent systematic error of about  $\pm 15\%$  in the  $\text{Re}(\sigma_{xx})$  taken from this formula. The determination of  $P_0$  produces an additional experimental uncertainty in  $\text{Re}(\sigma_{xx})$  for  $f > 2$  GHz. This “normalization error” varies strongly with  $f$  but is independent of  $B$  and  $T$ . We estimate it as to  $\pm 0.4$   $\mu\text{S}$  for  $f > 2$  GHz. The in-plane microwave electric field is largely confined to the slots, so  $\text{Re}(\sigma_{xx})$  characterizes the 2DES in the slots, where the antidot pattern exists.

At low  $B$ , both microwave transmission and dc magnetoresistance show the well-known commensurability oscillations<sup>5</sup> between the electron cyclotron radius and the period of the antidot array. Figure 1(b) shows 1 GHz microwave power  $P$  sent through the transmission line, vs  $B$  in the low magnetic field range. Electron geometric resonances appear for cyclotron orbits circling one and four antidots, indicating that in between the antidots there is low-disorder

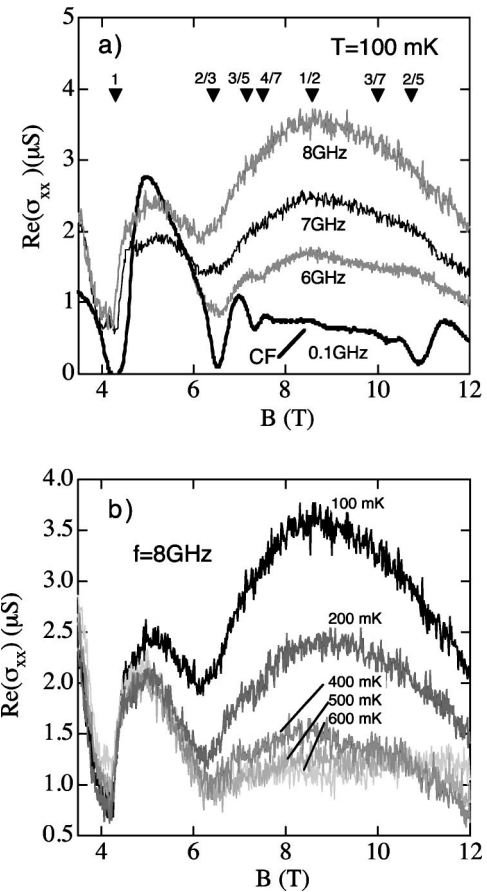


FIG. 2. Measured microwave conductivity  $\text{Re}(\sigma_{xx})$  vs magnetic field  $B$  for an antidot sample. Solid triangles indicate Landau-level filling factors,  $\nu$ . (a) 100 mK, various frequencies  $f$ . (b)  $f=8$  GHz, various temperatures.

2DES, characterized by mean free path  $\geq 3$   $\mu\text{m}$ .

We now focus on high magnetic fields, especially the range  $2/3 < \nu < 1/3$ , for which we obtained our main results. Figure 2(a) shows traces  $\text{Re}(\sigma_{xx})$  vs  $B$  for several frequencies  $f$ . At the lowest  $f$  of 0.1 GHz, the trace shows features well known from dc transport, with several dips in  $\text{Re}(\sigma_{xx})$  coming from the FQHE, including the 3/7 and 4/7 FQH states. Around  $\nu=1/2$  ( $B=8.5$  T), this trace exhibits a small peak which is marked “CF” in the figure, since it is likely an effect of the CF Fermi surface. This peak is absent in the sample without the antidots. We ascribe this small peak to the antidots or to residual disorder induced by the antidot lithography.  $\text{Re}(\sigma_{xx})$  vs  $B$  shows no geometric resonances corresponding to CF cyclotron orbits around antidots; observation<sup>6,7</sup> of these resonances requires lower disorder samples.

Our main result appears in the successively higher- $f$  traces of Fig. 2(a). Around 8.5 T, where  $\nu=1/2$ ,  $\text{Re}(\sigma_{xx})$  vs  $B$  develops a broad maximum, which dominates the conductivity at high  $f$ .  $\text{Re}(\sigma_{xx})$  clearly increases monotonically with  $f$  in the  $B$  range of this maximum from  $B$  just above the 2/3 FQHE minimum up to our highest  $B$  just below the 1/3 effect. The  $f$  dependence is more complicated for  $B$  just above the  $\nu=1$  integer quantum Hall effect (IQHE), where

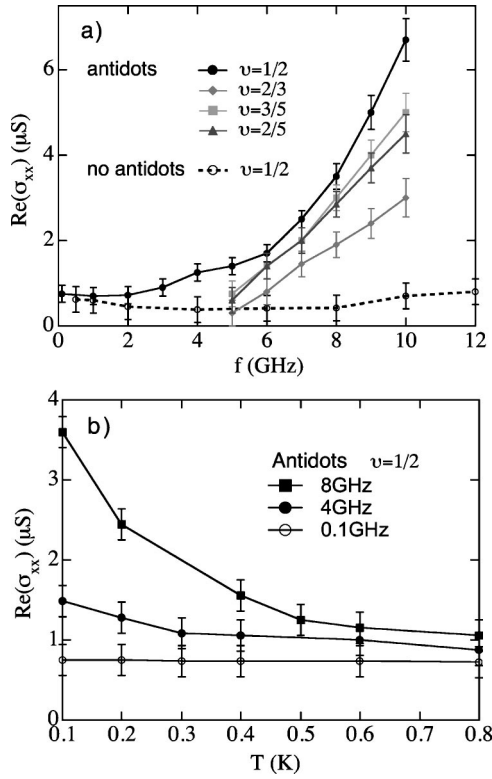


FIG. 3. Conductivity  $\text{Re}(\sigma_{xx})$  for sample with antidots (closed symbols) and  $\nu=1/2$ , and for sample without antidots (open symbols). (a)  $\text{Re}(\sigma_{xx})$  vs frequency  $f$  for various Landau fillings  $\nu$ . Data for  $\nu=2/3$ ,  $2/5$ , and  $3/5$  below 5 GHz are within error of 0  $\mu\text{S}$ , and are omitted for clarity. Lines are guides to the eye. (b)  $\text{Re}(\sigma_{xx})$  vs  $T$  at  $\nu=1/2$ , for several frequencies.

$\text{Re}(\sigma_{xx})$  apparently decreases with  $f$  between 0.1 and  $\sim 4$  GHz. The data in Fig. 2(b) show that the strong frequency response of the conductivity only exists for  $T < 0.5$  K. Figure 2(b) shows  $\text{Re}(\sigma_{xx})$  vs  $B$  for  $f=8$  GHz, measured at several temperatures. The broad  $\nu \sim 1/2$  maximum in  $\text{Re}(\sigma_{xx})$  vs  $B$  disappears gradually as the temperature is increased; the peak height is roughly halved at 200 mK, and the peak is unobservable at 600 mK.

In Fig. 2(a), the normalization error is small for the 0.1 GHz trace, and can only shift the other traces by  $B$ -independent constants, estimated to be within  $\pm 0.4$   $\mu\text{S}$ . Normalization error, which is independent of  $T$  as well as of  $B$  could uniformly shift all the curves together in Fig. 2(b) by  $\pm 0.4$   $\mu\text{S}$ .

Figure 3 summarizes the trends evident from Fig. 2.  $\text{Re}(\sigma_{xx})$  vs  $f$  at  $T \approx 100$  mK is plotted in Fig. 3(a) for  $\nu = 1/2, 2/3, 3/5$ , and  $2/5$ . For the reference sample lacking antidots (open symbols, dotted line), the error bars shown are mainly due to normalization error, and  $\text{Re}(\sigma_{xx})$  vs  $f$  is constant within this error. The strong  $f$  dependence is clearly associated with the antidots. Both the reference sample and the antidot sample have some  $f$  sensitivity at the edges of and around transitions between QHE minima, but only the antidot sample shows the increasing  $\text{Re}(\sigma_{xx})$  vs  $f$  in the  $1/3 < \nu < 2/3$  regime. The strong  $T$  dependence of the high  $f$  conductivity is summarized in Fig. 3(b).  $\text{Re}(\sigma_{xx})$  vs  $T$  is shown at

$\nu = 1/2$  ( $B = 8.5$  T) for  $f = 0.1, 4, 8$  GHz. For  $T > 0.5$  K, the conductivity is nearly the same at microwave frequencies and at 0.1 GHz. As  $T$  is decreased below 0.5 K, the contrast between low- $f$  and microwave conductivity is striking:  $\text{Re}(\sigma_{xx})$  is nearly  $T$  independent at low  $f$ , but at higher  $f$  increases strongly with decreasing  $T$ .

Delocalized carriers must exist between the antidots to cause the dc-limit conductivity, but cannot explain the  $T$ -dependence of the high- $f$  peak in  $\text{Re}(\sigma_{xx})$  vs  $B$ . The  $f$  dependent conductivity of delocalized carriers, such as CF's, is expected at least to some extent to follow a Drude model, with characteristic scattering time  $\tau$ . For the CF case at  $\nu = 1/2$ , the observed complex conductivity  $\sigma_{xx}$  is related to the CF conductivity  $\tilde{\sigma}_{xx}$  by  $\sigma_{xx} = \sigma_{1/2}^2 / \tilde{\sigma}_{xx}$ ,<sup>8</sup> where  $\sigma_{1/2} = 2e^2/h$ . The Drude model gives  $\tilde{\sigma}_{xx} = \tilde{\sigma}_{dc} / (1 + i\omega\tau)$ , where  $\omega = 2\pi f$ , so observed  $\sigma_{xx} = (1 + i\omega\tau)\sigma_{dc}$ . Thus,  $\text{Re}(\sigma_{xx})$  constant with  $f$  is called for by the Drude model for CFs, contrary to our experimental results on antidot lattices. Recent theoretical work<sup>12</sup> applicable to  $\nu = 1/2$  CF transport and to magnetic scattering of electrons in a disorder potential, points out corrections to the Drude model. For  $\omega\tau \ll 1$ , and weak random potentials, that theory predicts increasing  $\text{Re}(\sigma_{xx})$  vs  $f$  at  $\nu = 1/2$ .

As shown in Fig. 3(b), the low  $f$ ,  $\nu = 1/2$  conductivity is essentially  $T$  independent for  $T \lesssim 1$  K. Hence scattering that leads to dc resistance at  $\nu = 1/2$  is not causing the increase of  $\text{Re}(\sigma_{xx})$  at high  $f$ , which is strongly reduced even at 200 mK. In the corrected Drude models, or any model with mobile carriers, the time scale of scattering is a factor in dc conductivity, and is also characteristic of the finite  $f$  response. Since, as  $T$  decreases, the enhanced microwave conductivity emerges without being accompanied by any change in the dc-limit conductivity, it must arise from a conduction mechanism different from that responsible for dc transport.

Since the enhanced microwave absorption appears to be inconsistent with the dc-conducting states in between the antidots, and is not observed in the reference sample or in other 2DES samples lacking antidots,<sup>11</sup> it is natural to associate it with states at the antidot edges. In this case the observed  $f$  dependence would be that of the coupling of the microwave field with edge excitations. No peak in the spectrum is observed, so the measurement can be interpreted as a lossy dielectric response, effectively accessing just the low  $f$  tail of edge modes. Changes in the configuration of the edge states, or in their ability to dissipate microwave power would then be responsible for the  $T$  dependence of the observed high  $f$   $\text{Re}(\sigma_{xx})$ .

Because the microwave conductivity is  $T$  sensitive at such low  $T$ , it appears that the emergence of some correlated state must be associated with the  $T$  sensitivity. Such  $T$ -sensitive correlated states have been predicted<sup>17</sup> to exist at quantum Hall edges. The edge potential of the etched antidots in our sample must vary slowly on the scale of the magnetic length,  $(\hbar/eB)^{1/2}$ , and so is expected to undergo reconstruction into strips.<sup>17,18</sup> Because we observe well-defined FQHE states, there are apparently regions between the antidots that are well characterized by bulk states. The antidot depletion di-

ameter (150-250 nm) and lattice constant (500 nm) then constrain the length over which strips could develop.

The present experiment operates in a different regime than previous edge spectroscopy,<sup>3,13-16</sup> and may access edge modes of alternate type. The microwave frequency and temperature are lower than in FIR (Refs. 3 and 13) investigations, and the antidot edges are much shorter than the edges looked at in rf (Ref. 14) or pulsed experiments<sup>15,16</sup> on large QHE samples. Besides accessing large wave vectors, the smallness of the antidots can make the present measurement sensitive to modes that would be completely damped out on macroscopic edges.

While much is not understood about quantum-Hall edges, tunneling experiments<sup>19,20</sup> have revealed behavior of fractional-regime edges that matches the chiral Luttinger liquid description of FQHE edges,<sup>21</sup> and distinct, noninteracting Fermi liquid behavior of IQHE edges. Tunneling experiments measure I-V curves for tunneling into edges of QHE systems; the I-V curves contain a power-law regime, in which  $I \propto V^\alpha$ . Two features of the tunneling results may correlate with the present microwave data. First, like the microwave absorption the tunneling behaves differently in the fractional regime  $\nu < 1$  than it does at higher  $\nu$ . With  $\nu < 1$ ,  $\alpha$  takes the value  $(\nu^{-1} - 1)$ , as had been predicted for a

chiral Luttinger liquid based theory,<sup>21</sup> while  $\alpha$  is roughly unity for  $\nu > 1$ .<sup>19</sup> Second,  $\alpha$  has been observed to vary continuously according to this formula as  $\nu$  is swept.<sup>20</sup> This tunneling behavior holds continuously for a range of  $\nu$ , including 1/2, that is essentially the same as that for which we observe enhanced microwave absorption.

Finally, we cannot rule out more exotic states of the antidot edges as explanations of the low  $T$  microwave absorption. Edge modes coupled with phonons in the host semiconductor have been predicted theoretically,<sup>22</sup> and would likely be quite sensitive to  $T$ . Edge charge density waves (Wigner crystal) (Ref. 23) have been predicted to develop at QHE edges, and could be  $T$  sensitive. Coupling between edges of neighboring antidots could play a role in modes of an antidot array like that studied here.

In conclusion, we observe an anomalous microwave response vs  $f$  on antidot patterned 2DES at high magnetic fields. The observed  $T$  dependence suggests strongly that the effect is associated with the edges of the antidots.

We thank N. Bonesteel and Kun Yang for valuable discussions, and Jian Wang and Jie Yao for assistance. This work was supported by the Air Force Office of Scientific Research, and the National Science Foundation.

- 
- <sup>1</sup>W. Kohn, Phys. Rev. **123**, 1242 (1961).  
<sup>2</sup>S.J. Allen, Jr., D.C. Tsui, and R.A. Logan, Phys. Rev. Lett. **38**, 980 (1977).  
<sup>3</sup>K. Kern *et al.*, Phys. Rev. Lett. **66**, 1618 (1991); A. Lorke, J. Kotthaus, and K. Ploog, Superlattices Microstruct. **9**, 103 (1991); Y. Zhao *et al.*, Appl. Phys. Lett. **60**, 1510 (1992).  
<sup>4</sup>D.C. Tsui, H.L. Stormer, and A.C. Gossard, Phys. Rev. Lett. **48**, 1559 (1982).  
<sup>5</sup>D. Weiss *et al.*, Phys. Rev. Lett. **66**, 2790 (1991).  
<sup>6</sup>W. Kang *et al.*, Phys. Rev. Lett. **71**, 3850 (1993).  
<sup>7</sup>J.H. Smet *et al.*, Phys. Rev. B **56**, 3598 (1997).  
<sup>8</sup>B.I. Halperin, in *Perspectives in Quantum Hall Effects*, edited by S. Das Sarma and A. Pinczuk (Wiley, New York, 1996), p. 225; B.I. Halperin, P.A. Lee, and N. Read, Phys. Rev. B **47**, 7312 (1993).  
<sup>9</sup>H.L. Stormer and D.C. Tsui, in *Perspectives in Quantum Hall Effects* (Ref. 8), p. 385.  
<sup>10</sup>G.A. Vawter, in *Handbook of Advanced Plasma Processing Techniques*, edited by R. Shul and S. Pearton (Springer, Berlin, 2000), 507.  
<sup>11</sup>L.W. Engel, D. Shahar, Ç. Kurdak, and D.C. Tsui, Phys. Rev. Lett. **71**, 2638 (1993); also in *Physical Phenomena in High Magnetic Fields II, Proceedings* (World Scientific, Singapore, 1996) p. 23; L.W. Engel, C.-C. Li, D. Shahar, D.C. Tsui, and M. Shayegan, Solid State Commun. **104**, 167 (1997); C.-C. Li, J. Yoon, L.W. Engel, D. Shahar, D.C. Tsui, and M. Shayegan, Phys. Rev. B **61**, 10905 (2000).  
<sup>12</sup>J. Wilke *et al.*, Phys. Rev. B **61**, 13774 (2000).  
<sup>13</sup>T. Demel *et al.*, Phys. Rev. Lett. **64**, 788 (1990).  
<sup>14</sup>See, for example, I. Grodnensky, D. Heitmann, and K. von Klitzing, Phys. Rev. Lett. **67**, 1019 (1991); N.Q. Balaban *et al.*, Phys. Rev. B **55**, 13 397 (1997).  
<sup>15</sup>R.C. Ashoori *et al.*, Phys. Rev. B **45**, 3894 (1992).  
<sup>16</sup>G. Ernst *et al.*, Phys. Rev. Lett. **79**, 3748 (1997).  
<sup>17</sup>Xin Wan, Kun Yang, and E.H. Rezayi, Phys. Rev. Lett. **88**, 056802 (2002).  
<sup>18</sup>D.B. Chklovskii, B.I. Shklovskii, and L.I. Glazman, Phys. Rev. B **46**, 4026 (1992).  
<sup>19</sup>A.M. Chang, L.N. Pfeiffer, and K.W. West, Phys. Rev. Lett. **77**, 2538 (1996).  
<sup>20</sup>M. Grayson *et al.*, Phys. Rev. Lett. **80**, 1062 (1998).  
<sup>21</sup>X.G. Wen, Phys. Rev. B **41**, 12 838 (1990).  
<sup>22</sup>O. Heinonen and S. Eggert, Phys. Rev. Lett. **77**, 358 (1996).  
<sup>23</sup>Eyal Goldmann and Scot R. Renn, Phys. Rev. B **60**, 16 611 (1999); S.M. Reimann *et al.*, Phys. Rev. Lett. **83**, 3270 (1999).